



High-throughput acoustic separation of platelets from whole blood

Journal:	<i>Lab on a Chip</i>
Manuscript ID	LC-ART-05-2016-000682.R1
Article Type:	Paper
Date Submitted by the Author:	21-Jul-2016
Complete List of Authors:	Chen, Yuchao; The Pennsylvania State University, Department of Engineering Science and Mechanics Wu, Mengxi; Pennsylvania State University, Engineering Science and Mechanics Ren, Liqiang; The Penn state University, Department of Engineering Science and Mechanics Liu, Jiayang; Pennsylvania State University, Engineering Science and Mechanics Whitley, Pamela; American Red Cross Wang, Lin; Ascent Bio-Nano Technologies Inc., Huang, Tony Jun; The Pennsylvania State University, Department of Engineering Science and Mechanics



Lab on a Chip

ARTICLE

High-throughput acoustic separation of platelets from whole blood

Received 00th January 20xx,
Accepted 00th January 20xx

DOI: 10.1039/x0xx00000x

www.rsc.org/

Yuchao Chen,^a Mengxi Wu,^b Liqiang Ren,^a Jiayang Liu,^a Pamela H. Whitley,^c Lin Wang,^d and Tony Jun Huang^b

Platelets contain growth factors which are important in biomedical and clinical applications. In this work, we present an acoustic separation device for high-throughput, non-invasive platelet isolation. In particular, we separated platelets from whole blood at a 10 mL/min throughput, which is three orders of magnitude greater than that of existing acoustic-based platelet separation techniques. Without sample dilution, we observed more than 80% RBC/WBC removal & platelet recovery. High throughput, high separation efficiency, and biocompatibility make this device useful for many clinical applications.

Introduction

Platelets are micron-sized, disk-shaped cell fragments which constitute about 5% of cells in blood. They play a role in blood clots formation, as they seal breaks during hemostasis.¹ Platelets are part of physiological processes such as wound healing,² liver regeneration,³ tumor metastasis,⁴ and capturing bacteria for neutrophils.⁵ As a rich source of growth factors, platelets accelerate the recovery of bone and soft tissues. Platelets are transfused for chemotherapy, thrombocytopenia secondary to bone marrow neoplasms, and platelet function defects.^{6–8}

The gold-standard method for platelet separation is centrifugation, which separates platelets from other blood components by density. A whole blood sample is typically centrifuged at high speed (2,000–3,000 g) for approximately 10 mins. Centrifugation repeated over >1 hr yields a platelet concentrate for apheresis. However, the centrifugation-based method has limitations. Since platelets are activated by shear stress and aggregation,⁹ high-speed & repeated centrifugation activates the platelets, affecting their integrity and functionality. Metcalfe *et al.* showed that P-selectin expression, an indication of platelet activation, is 40% greater after centrifugation than a control.¹⁰ Others reported that 75% of platelet smears prepared by centrifugation showed altered morphologies, and that

centrifugation affected the release of B-thromboglobulin and platelet-derived growth factors.^{11–14} Moreover, it is difficult to remove white blood cells (WBCs) from platelets by centrifugation due to the similar densities of platelets and WBCs. If WBCs are mixed with platelets during transfusion, infection or immune repression may result. Transfusion currently demands an additional step called leukoreduction to remove WBCs by filters. This additional step prolongs the blood-processing time and affects the platelets' quality.¹⁵

Recent methods for platelet separation are based on microfluidic platforms, such as filtration, dielectrophoresis, and acoustics.^{16–25} Common to these microfluidic methods is low throughput (<< 1 mL/min), so they take a while to process a unit (~350 mL) of whole blood. In this regard, it is crucial to develop a new method for high-throughput, high-recovery-rate, high-biocompatibility, and high-purity platelet separation & enrichment, removing both red blood cells (RBCs) and WBCs in one step while preserving the integrity of the platelets.

In this work, we demonstrate an acoustic separation method to remove RBCs and WBCs from undiluted human whole blood. Experiments results show that this method yields high platelet recovery (>85%) and RBC/WBC removal (>80%) at a flow rate of 10 mL/min. Compared to the previous acoustic-based platelet separation,^{19,20} our throughput was increased by more than 2,500 times. We also conducted a comprehensive characterization on platelet integrity, including platelet activation level, morphology, and hypotonic shock response. Experimental results show excellent post-separation platelet integrity over conventional centrifugation methods. In addition, our acoustic separation method involves simple fabrication processes without complicated microfabrication techniques. With high throughput, high recovery rate, high purity, high

^aDepartment of Engineering Science and Mechanics, The Pennsylvania State University, University Park, PA, 16802, USA.

^bDepartment of Mechanical Engineering and Materials Science, Duke University, Durham, NC 27708, USA. E-mail: tony.huang@duke.edu

^cAmerican Red Cross, Mid-Atlantic Blood Services Region, 400 Gresham Dr., Suite 100, Norfolk, VA 23507, USA.

^dAscent Bio-Nano Technologies Inc., Durham, NC 27708, USA.

biocompatibility, and simplicity, our acoustic separation method is desirable for platelet enrichment upon transfusion.

Working Mechanism

Fig. 1A is a schematic of the acoustic-based platelet separation chamber. A thin reflective resonator is fabricated by bonding a composite transducer to the bottom of a stainless steel fluidic chamber. The chamber is much thinner than the transducer. Two inlets introduce a buffer at the upper level and a whole blood sample at the lower level. Fig. 1B shows the acoustic separation from a side view of the chamber. When the transducer operates at its resonance frequency, a pressure gradient is generated along the vertical direction with a pressure node (minimum) above the buffer solution and a pressure antinode (maximum) below the blood sample.^{26,27} As particles enter the pressure field, they are subject to acoustic radiation forces in the vertical direction.^{28–31}

$$F_r = -\left(\frac{\pi p_0^2 V_p \beta_m}{2\lambda}\right) \phi(\beta, \rho) \sin\left(\frac{4\pi x}{\lambda}\right) \quad (1)$$

$$\phi = \frac{5\rho_p - 2\rho_m}{2\rho_p + \rho_m} \frac{\beta_p}{\beta_m} \quad (2)$$

where p_0 , V_p , λ , ϕ , x , ρ_m , ρ_p , β_m , and β_p are pressure amplitude, particle volume, wavelength of acoustic waves, contrast factor, vertical distance from the pressure node, density of medium, density of particles, medium compressibility, and particle compressibility. When passing through the pressure field, the two layers of fluids start to contact. At the same time, the RBCs/WBCs are subject to stronger acoustic radiation forces than platelets due to their greater volumes (their difference in volume is much more significant than their difference in contrast factor),¹⁹ so they move into the buffer at the upper level and flow to the top outlet. The platelets remain at the

lower level of the chamber and flow to the bottom outlet. To reduce the mixing or contamination of the two fluids, dividers are incorporated into the channel to prevent the contact between the top and bottom fluids.

Before separation can work effectively, the mismatch of acoustic impedances between two fluids must be addressed.³² The acoustic impedance Z of a material is proportional to the speed of sound c in this material and the material density ρ : $Z = c\rho$. Sameer *et al.* reported that even a slight difference of acoustic impedances between two fluids (as low as 0.1%) can induce fluid relocation in a resonant acoustic field; the fluid of higher impedance moves to the node while the other fluid of lower impedance moves to the antinode.³² Typical acoustic impedances are 1.66×10^6 kg/(sec·m²) for blood and 1.48×10^6 kg/(sec·m²) for a water-based buffer such as $1 \times$ PBS solution. This mismatch is significant enough to move the entire blood sample including platelets into the top outlet, resulting in a low platelet recovery rate. To prevent fluid relocation during platelet separation, the acoustic impedance of the buffer may be adjusted until it is equal to or higher than that of the blood sample. Considering that aqueous dextrose (or glucose) is of higher acoustic impedance than blood (1.77×10^6 kg/(sec·m²) at 25% concentration) and is biocompatible with blood components at a low concentration, dextrose is used to tune the acoustic impedance of the buffer.

Materials and methods

The separation chamber was built with stainless steel. Seven stainless steel sheets (60×20 mm) of thickness $75 \mu\text{m}$ were cut with various patterns by laser cutting and were laminated into a fluidic chamber sealed with epoxy (8265S, J-B Weld, USA). The total thickness of the chamber was $525 \mu\text{m}$ and the inner channel height was $375 \mu\text{m}$. The width of the channel was 17 mm. Tubing (McMaster-Carr, USA) of inner diameter 2.5 mm was assembled at the inlets and outlets with tube fittings. A customized 1-3 composite transducer (TransducerWorks Inc., PA, USA) of thickness 1.7 mm was bonded to the bottom of the fluidic chamber with Devcon 5-minute epoxy to form a resonator.

To deliver the blood sample and buffer, the tubing was connected to a homemade peristaltic pump, which afforded a flow rate from 1 to 50 mL/min. A RF signal generator (E4422B, Agilent Tech, USA) and a power amplifier (100A250A, Amplifier Research, USA) provided a coherent AC signal. The resonance frequency of the composite transducer after bonding to the fluidic chamber was measured with a vector network analyzer (VNA 2180, Array Solutions, USA).

The whole blood sample for acoustic separation was purchased from Zen-Bio, Inc. and analyzed with a hematology analyzer (Ac-T diff2, Beckman Coulter, USA) before and after processing. A Megafuge 16R (Thermo Scientific, MA, USA) provided centrifugation. Dextrose 50% sterile solution from Durvet was added into $1 \times$ PBS buffer to tune the buffer's acoustic impedance. The platelets' functionality and quality were evaluated by the expression level of CD 62P (P-selectin), the morphology score, and the hypotonic shock response (HSR). The expression level of P-selectin on the platelets' surface was measured with a human sP-selectin immunoassay

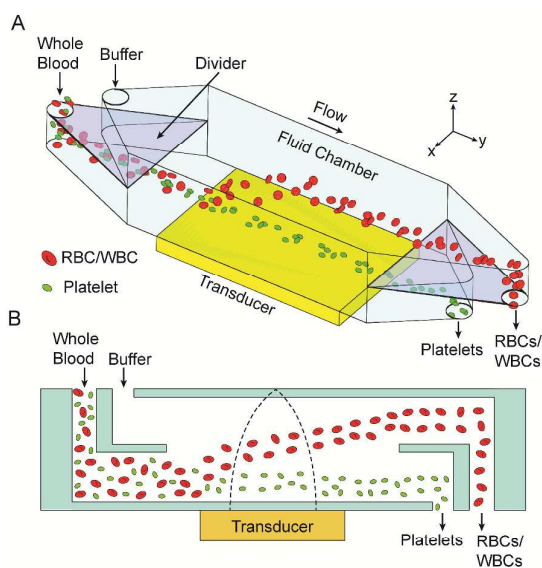


Fig. 1 (A) Schematic of the acoustic-based platelet separation device. (B) Side view of the device in the y-z plane.

(R&D Systems, Inc., MN, USA). The morphology score was characterized by a method developed by Wagner *et al.*^{33,34} Briefly, platelet samples were diluted with plasma to 300,000/ μL , and a drop (10 μL) was placed on a slide and examined under a microscope. 100 platelets were counted and evaluated according to 7 classes: disc, altered disc, ring, sickle cell, sphere, dendrite, and bizarre. The morphology score was then presented as the percentage of discoid platelets (discs and altered discs). The platelet hypotonic shock response (HSR) was measured turbidimetrically with an aggregometer (500VS, Chrono-Log, USA).

Results and Discussion

High-throughput separation

Conventional acoustophoresis devices separate cells/particles from the horizontal plane, so the channel width is restricted due to the limited cell/particle displacement.³⁵⁻⁴⁷ A typical channel width for acoustic separation is normally between 100 and 1000 μm , which results in a relatively small throughput (<1 mL/min). This is an obstacle for applications such as rare cell isolation and transfusion. To improve processing throughput without additional shear stress to cells, the channel dimensions are increased. By applying external forces along the vertical direction, the restriction in lateral channel width is lifted.⁴⁸ Shim *et al.* developed a dielectrophoretic field-flow-fractionation (DEP-FFF) technique by applying dielectric

forces along the vertical direction and increased the channel width to 25 mm.⁴⁹ This large channel dimension lead to a high processing throughput, which separated a 10 mL cell sample within 1 h.

We established a vertical acoustic separation configuration by generating acoustic radiation forces along the positive z axis at all positions inside the channel (Fig. 1). The channel was 17 mm in width, greater than the previous acoustophoresis channel by two orders of magnitude.⁵⁰⁻⁵⁹ Therefore, the throughput can be improved to ~ 10 mL/min without compromising the separation efficiency. Conventional microlithography was not ideal for fabricating this large, multi-layered flow channel. We developed a simple fabrication technique by laminating layers of laser-cut stainless steel slides into a single device. Moreover, to make fabrication easier, the thin reflector mode was adopted because it allows greater variation in layer thickness compared to the quarter-wave and half-wave resonant modes.

During platelet separation, the same flow rate was applied to both inlets. To prevent dilution of collected sample, a pump drew from the top outlet at this flow rate. The two fluids contacted each other only when they passed through the transducer's working region (20 mm in length), in order to minimize fluid diffusion. As shown in Fig. 2A, although a small fraction of blood cells was observed from the top outlet (right), most of the blood sample still came out the bottom (left) when the acoustic power was off. In contrast, when the acoustic power was on, a large number of RBCs/WBCs moved from the bottom to the top outlet as shown in Fig. 2B. The isolated

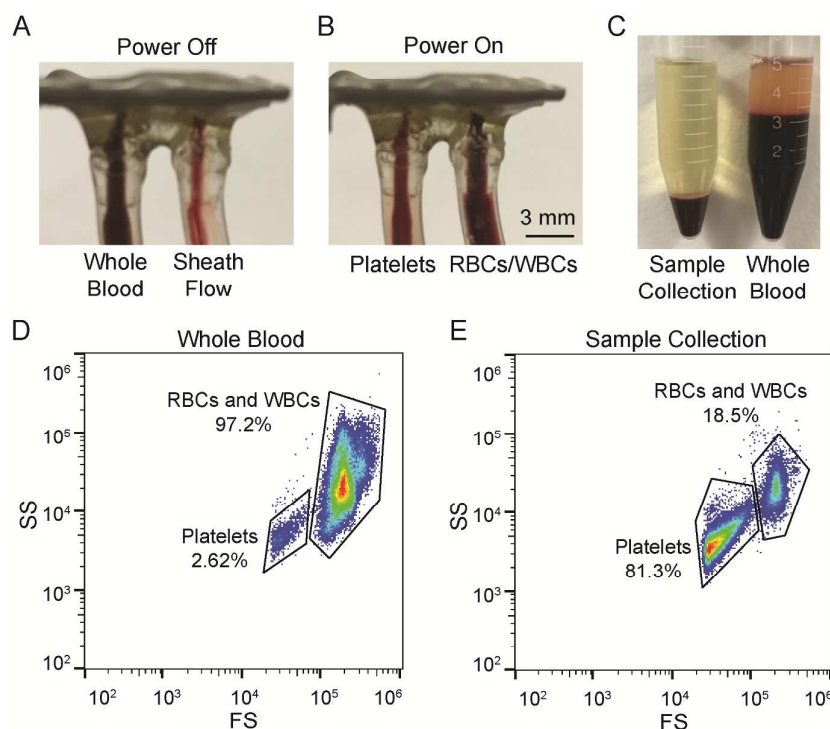


Fig. 2 Comparison of the device outlet when power was (A) off and (B) on. (C) Comparison of the isolated platelet sample collection (left) and whole blood sample (right). (D-E) Comparison of the flow cytometry results for whole blood and acoustically isolated platelet sample collection. SS: side scatter. FS: forward scatter.

platelet sample was collected from the bottom outlet to a centrifuge tube for comparison with the original whole blood sample. Fig. 2C shows 5 mL of collected sample (left) and original whole blood (right) after centrifugation at 300 g for 15 min. From the figure, more than 80% of the RBCs/WBCs were removed after acoustic separation. The blood samples were also analyzed by flow cytometry shown in Fig. 2D and Fig. 2E. Before separation (Fig. 2D), there was 97.2% of RBCs/WBCs and 2.6% of platelets in the blood sample. Significantly, the concentration of platelets was increased to 81.3% after separation (Fig. 2E) by reducing the RBCs/WBCs concentration to only 18.5%.

Tuning acoustic impedance

Since the acoustic impedance of undiluted whole blood is greater than that of $1\times$ PBS buffer (or other low-impedance buffers), the fluid relocation phenomenon prevents the isolation of platelets from RBCs/WBCs by moving the entire whole blood sample to the pressure node. As a result, it is necessary to engineer the buffer solution and match the acoustic impedance of the two fluids. In this work, dextrose was added to the buffer to tune its acoustic impedance. Fig. 3A shows the relation between resonance frequency and dextrose concentration. As the dextrose concentration increased from 0 to 15%, the resonance frequency also slightly increased from 225 to 237 kHz; this relation is approximated as linear.

RBC/WBC removal and platelet recovery are used to evaluate the performance of acoustic separation. Removal rate is defined as the ratio of blood cells collected from the top

outlet to the blood cells introduced at the inlet. The recovery rate is the ratio of isolated platelets collected from the bottom outlet to the platelets introduced at the inlet. As shown in Fig. 3B, the platelet recovery increased when dextrose was added to the buffer. At 15% dextrose concentration, the platelet recovery was 95.9%, meaning the fluid relocation was restrained. In contrast, RBC/WBC removal decreased as the dextrose concentration increased. As the medium density increased, the contract factor ϕ in Eq. (2) decreased, so the acoustic radiation force in Eq. (1) decreased. To balance recovery with removal rate, 10% dextrose in buffer solution was appropriate since both parameters were more than 80%.

Device performance

The input power was critical for acoustic separation efficiency. In a study of voltage applied to the transducer, the flow rate was set as 5 mL/min with 10% dextrose concentration. As shown in Fig. 4A, the RBCs/WBCs removal rate was significantly improved from 63.9% to 87.5% by increasing the applied voltage from 30 to 42 V_{pp} , thereby applying higher acoustic radiation forces to particles. The removal increased linearly in this voltage range. However, the rate of increase was much less at higher voltages. From 42 to 46 V_{pp} the removal increased less than 1%. This was because the transducer did not generate a stronger acoustic resonance. The influence of applied voltage to platelet recovery was not as significant to WBSs/RBCs removal. In the voltage range between 30 and 46 V_{pp} , the platelet recovery rate slightly decreased from 92.7% to 87.1%.

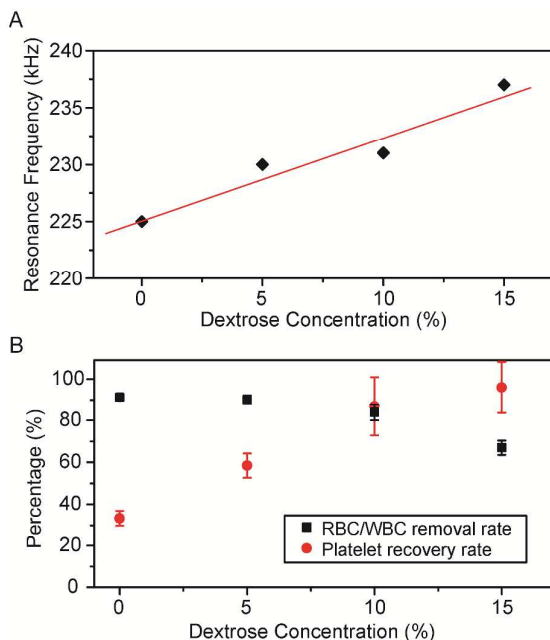


Fig. 3 (A) Relation between the device resonance frequency and dextrose concentration in buffer. (B) The influence of dextrose concentration upon the RBC/WBC removal and platelet recovery. The applied voltage was 46 V_{pp} and the flow rate was 5 mL/min.

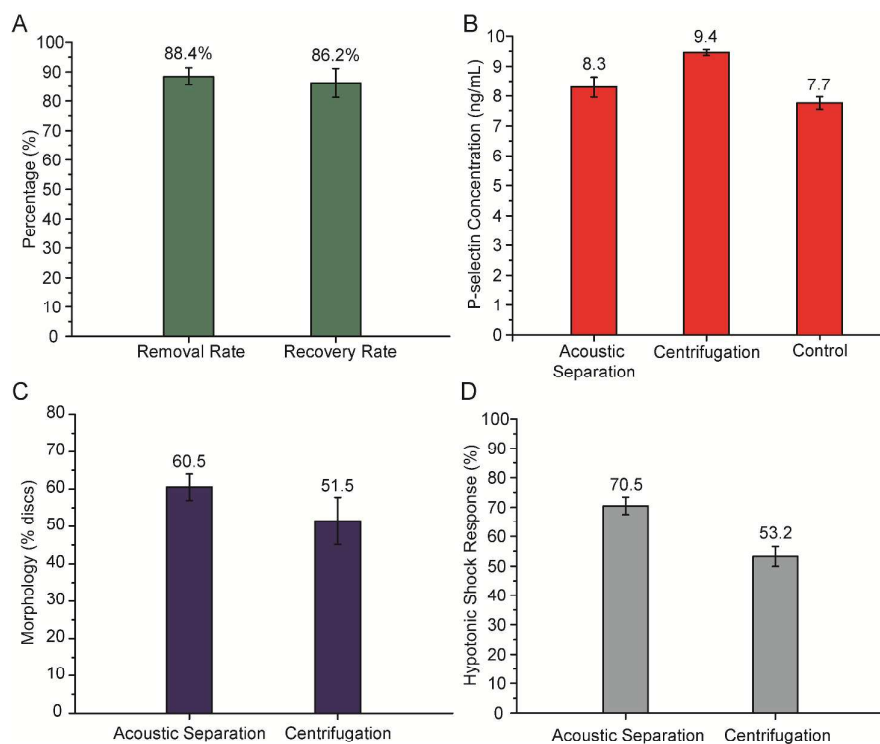


Fig. 5 (A) Separation performance at optimized conditions (46 V_{pp} applied voltage and 5 mL/min flow rate with a 10% dextrose concentration in the buffer solution). (B-D) Characterization of platelet functionality after isolation with our device and centrifugation, in terms of platelet activation level, morphology, and hypotonic shock response.

We also investigated the influence of flow upon separation performance. As flow speed increase, particles experience acoustic radiation force for a shorter period of time. Therefore, it is more difficult to remove RBCs/WBCs from platelets at a higher flow rate. Below a flow rate of 10 mL/min, the RBC/WBC removal rate and platelet recovery rate had small changes and both maintained above 80% (Fig. 4B). As the flow rate of blood sample increased from 2 to 10 mL/min, the RBC/WBC removal rate slightly decreased while the platelet recovery rate slightly increased. The device maintained good separation efficiency at this flow rate range, an improvement more than 2,500 times over the existing acoustic-based platelet separation techniques.^{19,20} When the flow rate further increased, the RBC/WBC removal rate fell below 80%. With our current device, the separation was optimized at 46 V_{pp} applied voltage, 5 mL/min flow rate, and a 10% dextrose concentration in the buffer to balance throughput, RBC/WBC removal, and platelet recovery. Fig. 5A shows that the separation yielded 88.4% RBC/WBC removal and 86.2% platelet recovery.

Platelet quality and function

Finally we compared our acoustic separation technique with conventional centrifugation in terms of post-separation platelet activation level, morphology, and hypotonic shock response (HSR)⁶⁰ (Fig. 5B-D). It seems that the acoustic separation device damaged the platelets much less than the centrifuge. In the latter method, the blood sample was first centrifuged at 300

g for 10 min. The top layer and middle layer were collected and centrifuged again at 2000 g for another 10 min to isolate

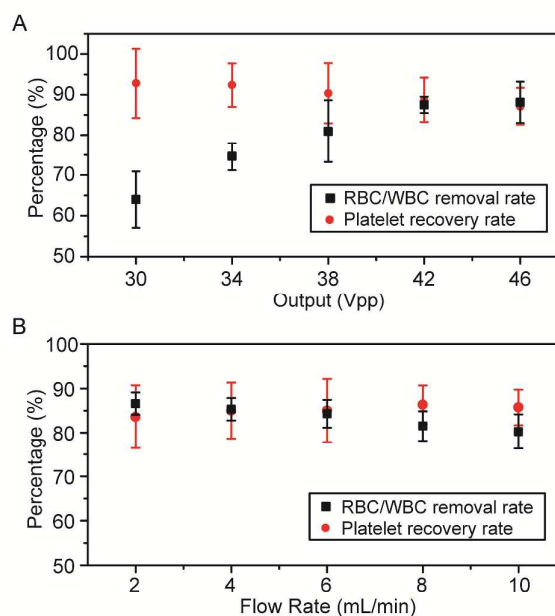


Fig. 4 The influence of (A) applied voltage and (B) flow rate to the separation performance in terms of RBC/WBC removal rate and platelet recovery rate.

platelets from RBCs/WBCs. The activation levels of the two methods were compared by measuring the expression level of CD 62P (P-selectin) as well as a control of untreated platelets in original whole blood. As shown in Fig. 5B, compared to the control sample the platelet activation level only increased 7.8% by acoustic separation, and 22% by centrifugation. The morphology score (Fig. 5C) was 60.5 for acoustic separation and 51.5 for centrifugation, indicating that discoid platelets were of greater integrity after acoustic separation than after centrifugation. Hypotonic Shock Response (HSR) measured the platelets' ability to extrude water after addition. The acoustically separated platelets had a higher HSR and so were of higher viability.

Conclusions

In this work, we separated platelets from undiluted whole blood with an acoustic separation device. High-throughput platelet separation along the vertical direction was achieved by introducing an acoustic resonator with simple device fabrication. To prevent fluid relocation, the acoustic impedance of the buffer solution was tuned with dextrose. We investigated the influence of applied voltage and flow rate to the separation efficiency. At a sample flow rate of 10 mL/min, we achieved greater than 80% RBC/WBC removal and platelet recovery. By optimizing experimental conditions such as applied voltage and buffer solution, we achieved 88.4% RBC/WBC removal and 86.2% platelet recovery at a throughput of 5 mL/min. Compared to centrifugation, our acoustic separation method preserves platelets with better integrity and functionality. Therefore, this method is a promising alternative for platelet isolation as well as other applications involving cell separation.

Acknowledgements

We gratefully acknowledge technical assistance from Drs. Andrey Skripchenko and Stephen J. Wagner and financial support from National Institutes of Health (R01 GM112048) and National Science Foundation (IIP-1534645 and IDBR-1455658). Components of this work were conducted at the Penn State node of the NSF-funded National Nanotechnology Infrastructure Network (NNIN).

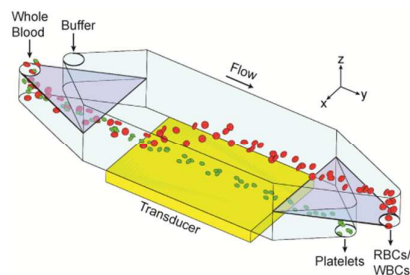
References

- 1 M. Leslie, *Science*, 2010, **328**, 562–564.
- 2 E. Artitua, I. Andia, and B. Ardanza, *Thromb. Haemost.*, 2004, **91**, 4–15.
- 3 M. Lesurtel, R. Graf, B. Aleil, and D. Walther, *Science*, 2006, **312**, 104–107.
- 4 L. Gay and B. Felding-Habermann, *Nat. Rev. Cancer*, 2011, **11**, 123–134.
- 5 S. Clark, A. Ma, and S. Tavener, *Nat. Med.*, 2007, **13**, 463–469.
- 6 B. L. Eppley, J. E. Woodell, and J. Higgins, *Plast. Reconstr. Surg.*, 2004, **114**, 1502–1508.
- 7 G. Intini, *Biomaterials*, 2009, **30**, 4956–4966.
- 8 R. Marx, *J. Oral Maxillofac. Surg.*, 2004, **62**, 489–496.

- 9 W. S. Nesbitt, E. Westein, F. J. Tovar-Lopez, E. Tolouei, A. Mitchell, J. Fu, J. Carberry, A. Fouras, and S. P. Jackson, *Nat. Med.*, 2009, **15**, 665–675.
- 10 P. Metcalfe, L. M. Williamson, C. P. Reutelingsperger, I. Swann, W. H. Ouwehand, and a H. Goodall, *Br. J. Haematol.*, 1997, **98**, 86–95.
- 11 M. J. H. Nagata, M. R. Messori, F. a C. Furlaneto, S. E. Cucini, A. F. Bosco, V. G. Garcia, T. M. Deliberador, and L. G. N. de Melo, *Eur. J. Dent.*, 2010, **4**, 395–402.
- 12 E. L. Snyder, a Hezzey, a J. Katz, and J. Bock, *Vox Sang.*, 1981, **41**, 172–177.
- 13 M. Merolla, M. a Nardi, and J. S. Berger, *Int. J. Lab. Hematol.*, 2012, **34**, 81–85.
- 14 L. Araki, M. Jona, H. Eto, N. Aoi, H. Kato, H. Suga, K. Doi, Y. Yatomi and K. Yoshimura, *Tissue Eng Part C Methods*, 2012, **18**, 176–185.
- 15 H. A. Phelan, J. L. Sperry and R. S. Friese, *J. Surg. Res.*, 2007, **138**, 32–36.
- 16 M. S. Pommer, Y. Zhang, N. Keerthi, D. Chen, J. A. Thomson, C. D. Meinhart, and H. T. Soh, *Electrophoresis*, 2008, **29**, 1213–1218.
- 17 N. Piacentini, G. Mernier, R. Tornay, and P. Renaud, *Biomicrofluidics*, 2011, **5**, 034122.
- 18 S. Choi, T. Ku, S. Song, C. Choi and J.-K. Park, *Lab Chip*, 2011, **11**, 413–418.
- 19 J. Nam, H. Lim, D. Kim and S. Shin, *Lab Chip*, 2011, **11**, 3361–3364.
- 20 J. Dykes, A. Lenshof, I.-B. Åstrand-Grundström, T. Laurell, and S. Scheduling, *Plos One*, 2011, **8**, e23074.
- 21 Y. Chen, P. Li, P.-H. Huang, Y. Xie, J. D. Mai, L. Wang, N.-T. Nguyen and T. J. Huang, *Lab Chip*, 2014, **14**, 626–645.
- 22 S.-C. S. Lin, X. Mao and T. J. Huang, *Lab Chip*, 2012, **12**, 2766–2770.
- 23 S. Li, X. Ding, Z. Mao, Y. Chen, N. Nama, F. Guo, P. Li, L. Wang, C. E. Cameron and T. J. Huang, *Lab Chip*, 2015, **15**, 331–338.
- 24 X. Ding, P. Li, S.-C. S. Lin, Z. S. Stratton, N. Nama, F. Guo, D. Slotcavage, X. Mao, J. Shi, F. Costanzo and T. J. Huang, *Lab Chip*, 2013, **13**, 3626–3649.
- 25 D. Ahmed, A. Ozcelik, N. Bojanala, N. Nama, A. Upadhyay, Y. Chen, W. Hanna-Rose and T. J. Huang, *Nature Communications*, 2016, **7**, 11085.
- 26 D. Carugo, T. Octon, W. Messaoudi, A. L. Fisher, M. Carboni, N. R. Harris, M. Hill and P. Glynne-Jones, *Lab Chip*, 2014, **14**, 3830–3842.
- 27 P. Glynne-Jones, R. J. Boltryk and M. Hill, *Lab Chip*, 2012, **12**, 1417.
- 28 H. Bruus, *Lab Chip*, 2012, **12**, 1014–1021.
- 29 K. Yosioka and Y. Kawasima, *Acustica*, 1955, **5**, 167–173.
- 30 C. R. P. Courtney, B. W. Drinkwater, C. E. M. Demore, S. Cochran, A. Grinenko and P. D. Wilcox, *Appl. Phys. Lett.*, 2014, **102**, 123508.
- 31 C. R. P. Courtney, C. E. M. Demore, H. Wu, A. Grinenko, P. D. Wilcox, S. Cochran and B. W. Drinkwater, *Appl. Phys. Lett.*, 2014, **104**, 154103.
- 32 S. Deshmukh, Z. Brzozka, T. Laurell and P. Augustsson, *Lab Chip*, 2014, **14**, 3394–3400.
- 33 S. J. Wagner, R. Vassallo, A. Skripchenko, M. Einarson, S. Seetharaman and G. Moroff, *Transfusion*, 2008, **48**, 1072–1080.
- 34 S. J. Wagner, A. Skripchenko, A. Myrup, D. Thompson-Montgomery, H. Awatefe and G. Moroff, *Transfusion*, 2010, **50**, 1028–1035.
- 35 J. Shi, H. Huang, Z. Stratton, A. Lawit, Y. Huang and T. J. Huang, *Lab Chip*, 2009, **9**, 3354–3359.
- 36 A. Lenshof and T. Laurell, *Chem. Soc. Rev.*, 2010, **39**, 1203–1217.

- 37 P. Augustsson, C. Magnusson, M. Nordin, H. Lilja and T. Laurell, *Anal. Chem.*, 2012, **84**, 7954–7962.
- 38 X. Ding, Z. Peng, S.-C. S. Lin, M. Geri, S. Li, P. Li, Y. Chen, M. Dao, S. Suresh and T. J. Huang, *Proc. Natl. Acad. Sci. U. S. A.*, 2014, **111**, 12992–12997.
- 39 L. Ren, Y. Chen, P. Li, Z. Mao, P.-H. Huang, J. Rufo, F. Guo, L. Wang, J. P. McCoy, S. J. Levine and T. J. Huang, *Lab Chip*, 2015, **15**, 3870–3879.
- 40 G. Yu, X. L. Chen and J. Xu, *Soft Matter*, 2011, **7**, 10063–10069.
- 41 J. Xu and D. Attinger, *Phys. Fluids*, 2007, **19**, 108107.
- 42 P. P. Austin Suthanthiraraj, M. E. Piyasena, T. A. Woods, M. A. Naivar, G. P. Lopez, and S.W. Graves, *Methods*, 2012, **57**, 259–271.
- 43 M. E. Piyasena, P. P. Austin Suthanthiraraj, R.W. Applegate Jr., A. M. Goumas, T. A. Woods, G. P. López, and S. W. Graves, *Anal. Chem.*, 2012, **84**, 1831–1839.
- 44 G. Destgeer, and H. J. Sung, *Lab Chip*, 2015, **15**, 2722–2738.
- 45 M. M. Katasonov, H. J. Sung, and S. P. Bardakhanov, *J. Eng. Thermophys. Rus.*, 2015, **24**, 36–56.
- 46 J. M. Gao, J. Carlier, S. X. Wang, P. Campistron, D. Callens, S. S. Guo and X. Z. Zhao, *Sens Actuators B Chem.*, 2013, **177**, 753–760.
- 47 M. Z. Ke, Z. Y. Liu, P. Pang, W. G. Wang, Z. G. Cheng, J. Shi, X. Z. Zhao and W. J. Wen, *Appl. Phys. Lett.*, 2006, **88**, 263505.
- 48 J. D. Adams, C. L. Ebbesen, R. Barnkob, A. H. J. Yang, H. T. Soh and H. Bruus, *J. Micromech. Microeng.*, 2012, **22**, 075017.
- 49 S. Shim, K. Stenke-Hale, A. M. Tsimberidou, J. Noshari, T. E. Anderson and P. R. C. Gascoyne, *Biomicrofluidics*, 2013, **7**, 011807.
- 50 P. Li, Z. Mao, Z. Peng, L. Zhou, Y. Chen, P.-H. Huang, C. I. Truica, J. J. Drabick, W. S. El-Deiry, M. Dao, S. Suresh and T. J. Huang, *Proc. Natl. Acad. Sci. U. S. A.*, 2015, **112**, 4970–4975.
- 51 F. Petersson, L. Aberg, A.-M. Sward-Nilsson and T. Laurell, *Anal. Chem.*, 2007, **79**, 5117–5123.
- 52 P. Thevoz, J. D. Adams, H. Shea, H. Bruus and H. T. Soh, *Anal. Chem.*, 2010, **82**, 3094–3098.
- 53 L. Y. Yeo, and J. R. Friend, *Annu. Rev. Fluid Mech.*, 2014, **46**, 379–406.
- 54 L. Y. Yeo, H. C. Chang, P. P. Y. Chan, and J. R. Friend, *Small*, 2011, **7**, 12–48.
- 55 L. Y. Yeo, and J. R. Friend, *Biomicrofluidics*, 2009, **3**, 012002.
- 56 T. Franke, S. Braunmüller, L. Schmid, A. Wixforth, and D. A. Weitz, *Lab Chip*, 2010, **10**, 789–794.
- 57 L. Schmid, D. A. Weitz, and T. Franke, *Lab Chip*, 2014, **14**, 3710–3718.
- 58 R. Guldiken, M. C. Jo, N. Gallant, U. Demirci, and J. Zhe, *Sensors*, 2012, **12**, 905–922.
- 59 Z. Wang, and J. Zhe, *Lab Chip*, 2011, **11**, 1280–1285.
- 60 Y. Kececi, S. Ozsu and O. Bilgir, *Wounds*, 2014, **26**, 232–238.

Graphical Abstract



An acoustic separation device that can achieve high-throughput, high-efficiency, and non-invasive platelet enrichment from undiluted whole blood.